

Fermi National Accelerator Laboratory

FERMILAB-Conf-91/268-E

Measurement of the $\bar{p}p$ Total Cross Section at $\sqrt{s} = 1800$ GeV

S. White, *Rockefeller University*
for the CDF Collaboration

Fermi National Accelerator Laboratory
P.O. Box 500, Batavia, Illinois 60510

October 1991

* Presented at the *Fourth International Conference on Elastic and Diffractive Scattering*, La Biodola, Elba, Italy, May 22-25, 1991.



Operated by Universities Research Association Inc. under contract with the United States Department of Energy

A Measurement of the $\bar{p} p$ total cross section at $\sqrt{s} = 1800 \text{ GeV}$

Sebastian White, Rockefeller University
for the CDF Collaboration

Abstract

The pp differential elastic scattering cross section was measured at $\sqrt{s} = 1800 \text{ GeV}$, using an improved accelerator luminosity determination and CDF small angle data in the range of $0.05 \leq t \leq 0.2 (\text{GeV}/c)^2$. By extrapolating the differential cross sections to $t=0$ and using the optical theorem we obtain a total cross section of $\sigma_{tot}(pp) = 72.0 \pm 3.6 \text{ mb}$. This result is preliminary in the sense that we expect to further reduce the systematic error on the optical point.

1 Introduction

The goal of the CDF small angle physics program is to measure the diffractive processes of elastic scattering, diffraction dissociation and $\sigma_{tot}(\bar{p}p)$ at $\sqrt{s}=1800 \text{ GeV}$ [1]. For this purpose CDF data were recorded during special stores with high- β optics ($\beta \sim 72 \text{ m}$), using triggers derived from small angle detectors sensitive to the leading particles, mounted in Roman Pots.

In this paper we present results from the analysis of elastic scattering data recorded during one such store.

In the past year we also completed a study of the accelerator luminosity calibration in collaboration with the Fermilab accelerator department [2]. This work is described briefly in section 5 and has resulted in an improved luminosity measurement.

Independent of the total cross section measurement, we find that the effective cross section seen by the CDF minimum bias trigger, which is primarily sensitive to non-diffractive inelastic events, increases by a factor of 1.30 ± 0.06 in the energy range $546 \leq \sqrt{s} \leq 1800 \text{ GeV}$. This increase is small enough to constrain estimates of mini-jet production at our energy [3].

2 Method

We measure the differential pp elastic scattering cross section

$$\frac{d\sigma^{el}}{dt} = \left(\int L \right)^{-1} \frac{dN^{el}}{dt} \quad (2.1)$$

where

$$A \simeq p_{beam}^2 \cdot \theta_{final}^2$$

and the scattering angle, θ_{final} , was measured with bi-dimensional detectors at various 'stations' in the Tevatron.

The measured differential elastic scattering distribution was extrapolated to $t=0$ and the total cross section was calculated using the optical theorem:

$$\sigma_{tot}^2 = 16\pi(hc)^2(1 + \rho^2)^{-1} \frac{d\sigma^{el}}{dt} \Big|_{t=0} \quad (2.2)$$

A preliminary measurement of ρ has been presented at this conference [4]. We used a value $\rho=0.145$ (consistent with [4]) to obtain $\sigma_{tot} = 72.0 \pm 3.6 \text{ mb}$. It should be noted that our determination of σ_{tot} using eqn. 2.2 changes by only $\pm 1\%$ for $0.1 < \rho < 0.2$.

2.1 Track Measurement

The detector stations were located in non-cryogenic insertions of the Fermilab Tevatron beyond the CDF low- β quadrupole magnets. A simplified plan view of the CDF forward spectrometers is shown in figure 1.

tector stations. The trigger scintillators, which measured 3.33×2.70 cm in x and y , determine the geometrical acceptance of the spectrometer.

The efficiency of this trigger was calculated using events recorded during the same run with different trigger requirements and found to be 0.98 ± 0.01 .

In the data analysis, we determined the number of true elastic scattering events in the above data sample, used the high redundancy arising from the large number of measurements in the tracking to determine possible reconstruction losses and applied straightforward geometrical acceptance corrections to determine the differential spectrum of elastic events. In this analysis only DWC hits were used in reconstruction, although Si Strip detectors played a crucial role in the chamber calibration determining drift and delay line velocities.

For p trajectory reconstruction in the x - z plane, track segments found in Station 1 & 2 were used to determine the momentum and scattering angle of the p (using the interaction point as a constraint on the fit). The proton scattering angle was also determined using equation 2.3 and the location of the track segment in Station 6. We then plot the collinearity,

$$\delta\theta^x = \theta_p^x - \theta_{\bar{p}}^x \quad (2.4)$$

for all events (see figure 3a). There is a clear peak in collinearity with $\sigma_{\delta\theta^x} = 20 \mu\text{rad}$ in agreement with the calculated resolution for elastic events. There is also a substantial background whose shape is not, a priori, known.

To determine the number of signal events in the peak we performed fits to an assumed flat background + gaussian signal and compared to similar fits when further cuts were applied in which

1. an 'inelastic cut' was applied removing events with extra tracks in the event (fig. 3b) and
2. a further cut impact parameter, x_0 , calculated using S_1 & S_3 hits and assuming 900 GeV track momentum to extrapolate to the interaction point (fig. 3c).

Events plotted in figure 3c had a $3\text{-}\sigma$ cut applied on x_0 , where $\sigma_{x_0} = 0.056$ cm. Fits to these 2 distributions gave a

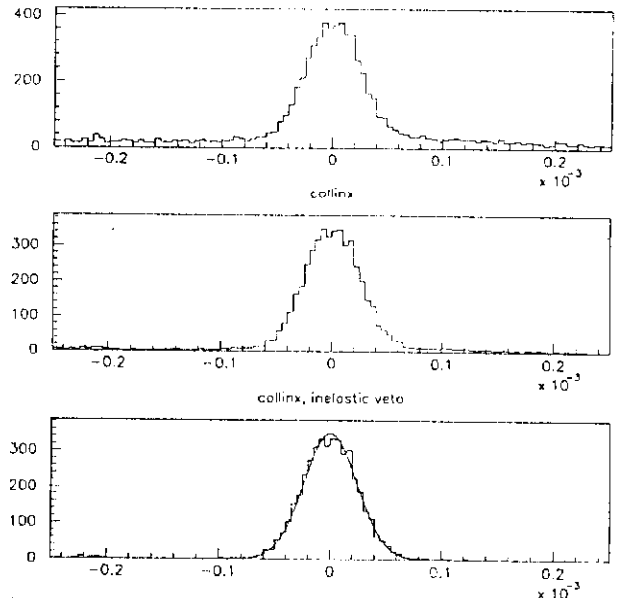


Figure 3: Collinearity of p and \bar{p} tracks in the x - z plane for a) all events, b) with inelastic veto and c) with a vertex cut.

consistent determination of the number of elastic events with the uncut sample, taking into account the efficiencies of cuts 1 & 2. Nevertheless, a systematic uncertainty of ± 200 events has been conservatively assigned to the number of events given in table 1 to reflect present uncertainty in these efficiencies [6].

Table I. Elastic Event Classification

event class	number of events
track segments in S_1, S_2, S_6 found	4332 +/- 80
missing S_1 or S_2	100 +/- 13
missing S_6	133 +/- 14
missing both segments	15 +/- 6
extra segments	225 +/- 100

Events for which no collinear elastic candidate was found according to the method described above were refit using track segments from stations S_3 and S_7 and a new collinearity variable was plotted. This second reconstruction path was also used to estimate further (negligible) reconstruction losses. Table 1 summarizes the classification of elastic events according to whether they were found in the primary reconstruction path, retrieved with stations 3 and 7 because of tracking inefficiency, or retrieved because

extra track segments were found in the event (usually due to upstream interactions).

Elastic candidates satisfying collinearity cuts on θ_x and θ_y were binned in t and the distribution was corrected for trigger and reconstruction efficiency.

A geometrical acceptance correction was applied to events in each t -bin taking into account the limited coverage of the detectors in azimuth.

The corrected differential elastic scattering rate was divided by the integrated Luminosity of $(1.24 \pm 0.08) \cdot 10^{30}$ and is plotted in figure 4. The data are well described by a simple exponential dependence on t , whose coefficient is found to be,

$$b = 16.5 \pm 0.5(\text{statistical})(\text{GeV}/c)^2 \quad (2.5)$$

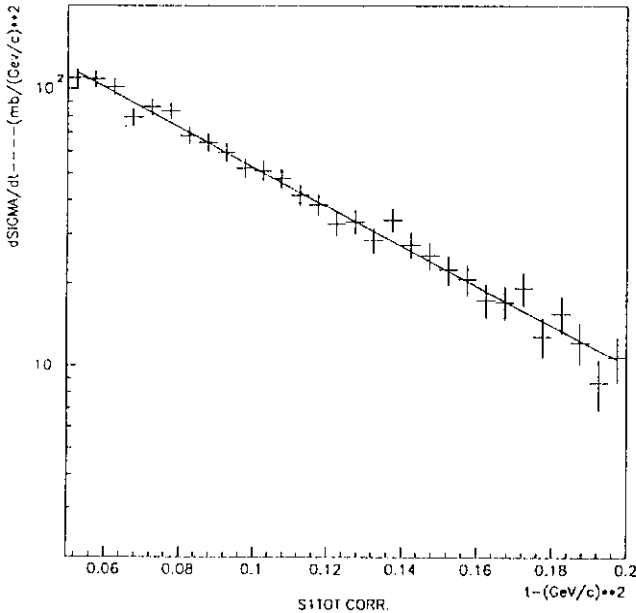


Figure 4: *Differential elastic scattering cross section. Data from Arm 0 and Arm 1 are combined.*

3 Systematic Errors on the Optical Point

We now consider the remaining systematic errors on the optical point measurement.

The contribution from possible errors in the effective lengths was found to be less than 3%. We used the relative alignment of detectors with elastic tracks to find the

maximum possible discrepancy from measured positions. Then a simple Monte Carlo calculation was used to find the effect of these discrepancies on the optical point.

Luminosity and the beam trajectory are discussed in more detail below.

The beam trajectory affects the elastic scattering distribution in the following sense. Our internal alignment of the detectors within the spectrometers using elastic tracks doesn't constrain the overall angle of the apparatus relative to the beam direction. On the other hand, such an offset would change the relative rate in detectors on either side of the beam, giving rise to 2 different elastic cross sections. Intuitively we expect this effect to partly cancel when data from both sides (Arm0 and Arm1) are combined.

3.1 Beam tilt angle

The beam tilt angle is determined by comparing data in the 2 spectrometer arms. This is done by starting with an angle $+\delta$ for a possible offset and then rebinning in terms of a new t variable.

$$t' = t_0 + 2 \cdot p^2 \cdot (\theta_x \cdot \delta) \quad (3.1)$$

A new acceptance, is also calculated for each spectrometer arm and the resulting corrected t -distribution is fitted to the form:

$$\frac{dN^{t'}}{dt} = \epsilon^A \cdot e^{bt} \quad (3.2)$$

The fitted total number of events is then:

$$N^{t'} = \epsilon^A / b \quad (3.3)$$

The elastic cross section integrated from $0.05 \leq t \leq 0.2(\text{GeV}/c)^2$ is plotted for Arm 0 and Arm 1 data in figure 5 using different choices for the beam tilt angle. Clearly the best choice for the beam tilt angle is in the range $-5.0 \mu r \leq \delta \leq 0.0 \mu r$.

When data from both arms are averaged, the fitted slope and intercept parameters (b and $\frac{d\sigma_{\text{elastic}}}{dt} |_{t=0}$) are insensitive to δ well beyond its possible range of uncertainty. This is evident from figure 6, which show the dependence of the fitted intercept on the beam tilt angle.

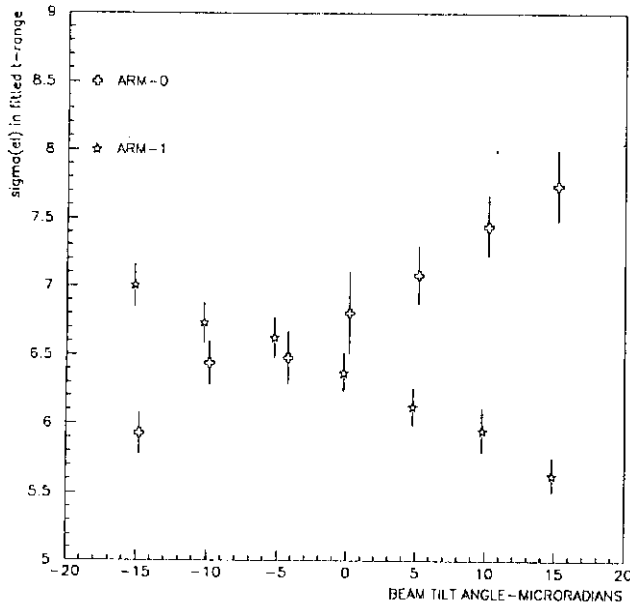


Figure 5: Elastic scattering cross section integrated over the range $0.05 \leq t \leq 0.2(\text{GeV}/c)^2$ vs. the assumed beam tilt parameter.

The statistical error on σ_{el} is $\pm 1.5\%$. Combining uncertainties from Luminosity ($\pm 6.8\%$), reconstruction losses and background ($\pm 3.0\%$) and trigger efficiency ($\pm 1.0\%$) we obtain

$$\sigma_{el} = 16.5 \pm 1.3 \text{ mb.} \quad (3.4)$$

4 The Total Cross Section

The optical theorem can now be used to derive $\sigma_{tot}(\bar{p}p)$ from the fit parameters to figure 4 yielding

$$\begin{aligned} \sigma_{tot}^2 &= 16\pi(\hbar c)^2(1 + \rho^2)^{-1} \frac{d\sigma^{el}}{dt} \Big|_{t=0} \\ &= 19.53 \cdot (1 + (.145)^2)^{-1} \\ &\quad \cdot ((271.0 \pm 13.1 \pm 23.7) \frac{\text{mb}}{(\text{GeV}/c)^2}) \\ \sigma_{tot} &= 72.0 \pm 3.6 \text{ mb} \end{aligned} \quad (4.1)$$

The errors contributing to the overall uncertainty in the optical point are listed separately in equation 4.1. The (second) systematic error results from the combined uncertainties from Luminosity, background/reconstruction efficiency, and trigger efficiency.

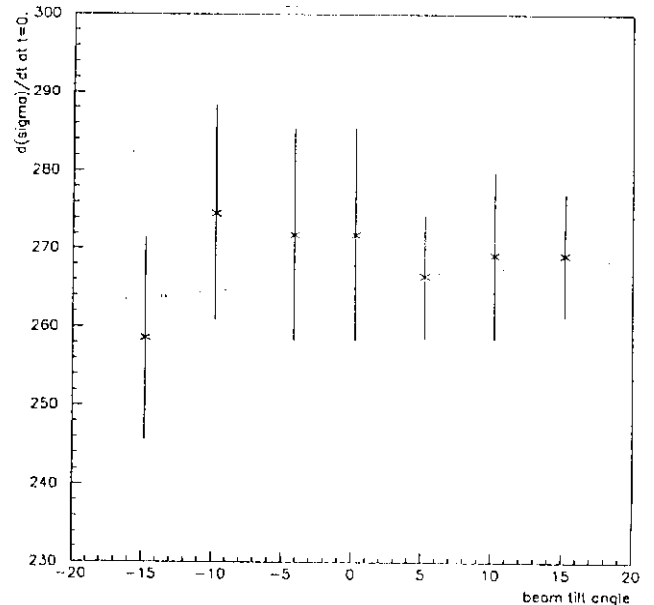


Figure 6: Dependence of the optical point (data from both spectrometer arms combined) on the assumed beam tilt parameter.

5 Luminosity Calibration and the Inelastic Cross Section

The instantaneous luminosity from stored p and \bar{p} beams in the Tevatron can be calculated from accelerator based measurements of bunch intensity and emittance and the known betatron amplitude and momentum dispersion at a given interaction region. This calculation is estimated to be accurate to $\pm 11\%$ and the dominant uncertainty comes from the bunch intensity measurements [7].

We have reduced this luminosity uncertainty by using data taken with the CDF detector at $\sqrt{s}=546$ GeV with a minimum bias trigger and comparing our measured inelastic cross section with that of UA4. This independent check on the luminosity, when combined with the accelerator calculation, reduced the uncertainty to $\pm 5.6\%$ at 546 GeV. The relative luminosity error when the beam energy was increased to $\sqrt{s}=1800$ GeV was found to be $\pm 4.3\%$. Hence an overall luminosity uncertainty of $\pm 6.8\%$ was assigned to our integrated luminosity at full beam energy.[2]

5.1 Minimum Bias Cross Section

The CDF minimum bias trigger requires at least 1 charged track in each of 2 sets of Beam-Beam counters (BBC's) covering the pseudorapidity range $3.3 \leq \eta \leq 5.9$ on either side of the interaction point.

This trigger is primarily sensitive to nondiffractive inelastic events and is nearly identical in coverage to the UA4 double arm trigger which spans pseudo rapidities of $3.0 \leq \eta \leq 5.6$ [8].

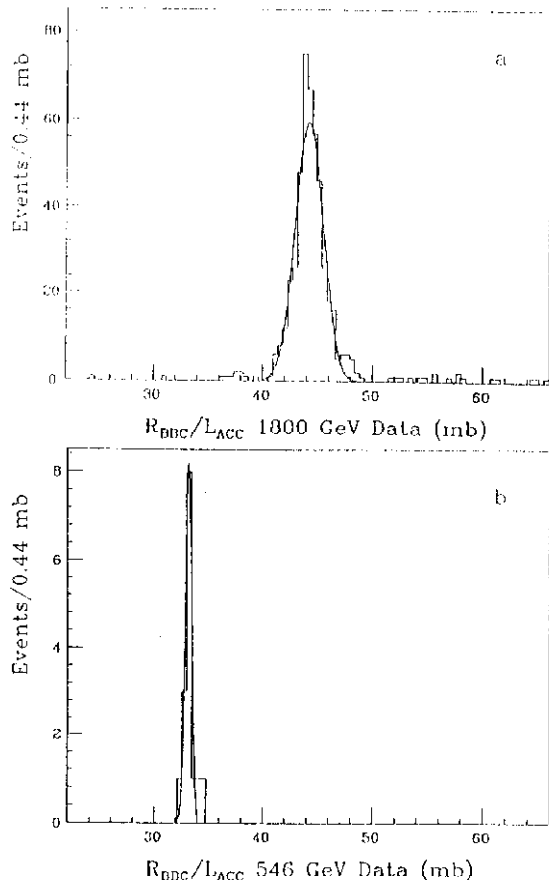


Figure 7: Determination of the minimum bias trigger (BBC) effective cross section from luminosity scaling, described in the text.

Figure 7b shows the rate of BBC counts divided by the uncorrected luminosity calculation. Data points correspond to accelerator measurements of the stored beam parameters called "flying wire scans" which are made periodically during CDF data taking. The expected rate for this trigger was calculated from the UA4 double arm cross section and used to correct the accelerator luminos-

ity scale. Based on a detailed study comparing accelerator calculations with observed rates and event vertex distributions under a variety of beam conditions we assigned an error to the relative luminosity at different collider running energies.

The corresponding cross section at $\sqrt{s}=1800$ GeV (shown in fig. 7a) increases by 1.30 ± 0.06 .

Independent of the elastic and total cross section measurements discussed above, this direct measurement of the increase of the 'minimum bias' cross section limits possible new thresholds in the inelastic cross section. For example, calculations of QCD mini-jet cross sections [3] predict an increase of 23-44 mb in our energy range, a rather dramatic increase compared to our observed rise of ~ 10 mb for either the total inelastic or 'minimum bias' cross sections.

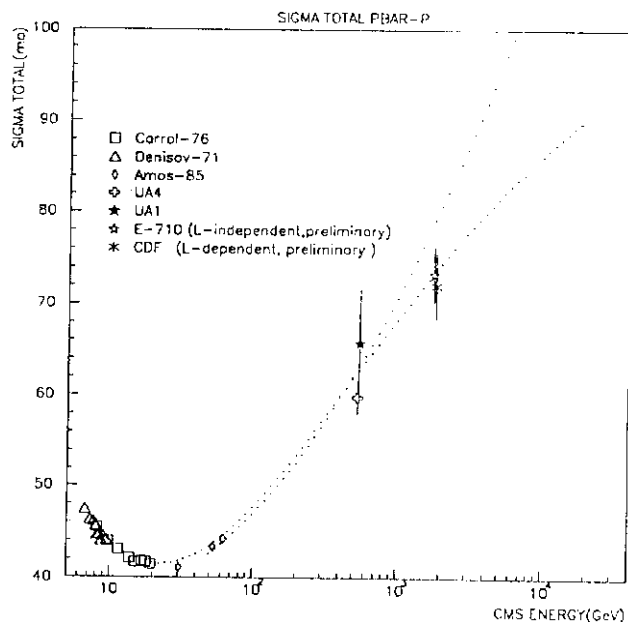


Figure 8: $P - P$ total cross section vs. CMS Energy.

6 Conclusion

We have measured $\sigma_{tot}(\bar{p}p) = 72.0 \pm 3.6$ mb. at $\sqrt{s}=1800$ GeV using an improved accelerator luminosity calibration and CDF elastic data. Our result is consistent with the value reported by E710 and smooth (roughly as $\ln s$) [9] extrapolations from lower energies as can be seen from fig-

ure 8.

Using an independent measurement of the rise of the inelastic cross section in the range $546 \leq \sqrt{s} \leq 1800$ GeV an increase by a factor of 1.30 ± 0.06 was found which restricts possible new thresholds in the inelastic cross section.

References

- [1] for further details on the CDF small angle apparatus see contribution by G.Apollinari in Proceedings of the Third International Conference on Elastic and Diffractive Scattering (Nucl.Phys.B(Proc.Supp)12 (1990)p12 and S.White in Elastic and Diffractive Scattering II, Editions Frontieres(1988) p27.
- [2] "CDF Luminosity Calibration" ,C.Pilcher and S.White , Fermilab preprint FN-550.
- [3] "QCD minijet cross sections", I.Sarcevic,S.D.Jellis and P.Carruthers, Phys.Rev.D 40 (1989) 1446.
- [4] "Status Report on E710", presented by S. Shukla, these proceedings.
- [5] The Tevatron beam energy has a systematic uncertainty of only ± 0.9 GeV at $\sqrt{s} = 1800$ GeV. See contribution by Roland Johnson in the proceedings of the 1988 CERN-US joint accelerator school.
- [6] We expect a more refined analysis, currently in progress, using both DWC and silicon hits to yield a smaller systematic error. This is likely to reduce the error on σ_{tot} from 5% to 4%.
- [7] N.Gelfand, "Computation of Tevatron Luminosity using measured Machine parameters" ,FN-938 (1990)
- [8] Phys. Lett. 147B (1984) 392. UA1 finds that $82.7 \pm 0.8\%$ of inelastic events satisfy their double arm trigger.
- [9] M.Block and R.Cahn, Phys.Lett.188b (1987) p.143. Fits 5 and 6 are plotted in figure 8.